Critical Flow of Liquid-Vapor Mixtures

JAMES E. CRUVER and R. W. MOULTON

University of Washington, Seattle, Washington

A unified theory of one-dimensional, adiabatic, separated, two-phase flow is presented. To describe the flow adequately, four mixture specific volumes are defined. They are based on area, momentum, kinetic energy, and velocity averages. Increasing relative velocity between the phases initially lowers all mixture specific volumes except the velocity average. The momentum average specific volume minimizes when the slip ratio equals $(V_g/V_f)^{1/2}$, while the kinetic energy average specific volume reaches its minimum value at a slip ratio of $(V_g/V_f)^{1/3}$. Area average specific value does not minimize with slip ratio.

Because a higher slip ratio would decrease the entropy of a closed system, $(V_g/V_f)^{1/3}$ is the maximum slip ratio attainable in two-phase critical flow. Based on the maximum slip ratio and isentropic flow, a new critical flow model was developed and compared with the steam-water critical flow data of four recent investigations. While the predicted flow rates followed well the pressure behavior of the experimental data, they were too low at high qualities and too high at low qualities. The average percentage difference between experimental and predicted critical flow rates was —8.5% (three hundred and seventy-six data points).

Differences in the approach to critical flow between a gas and a vapor-liquid stream appear to be caused by the latter's increased frictional and gravitational pressure drops and relative velocity effects.

A liquid-vapor stream exhibits a critical flow phenomenon similar to, but not identical with, that of a gas. Critical flow in a gas is described by $G = \sqrt{-g_c\left(\frac{\partial P}{\partial V}\right)_S}$, and is related to the velocity of sound in the same medium. Maximum flow rate and critical pressure are reached when the stream velocity is equal to that of a rarefaction wave in a gas. Because of this, the downstream pressure cannot be transmitted upstream and a back pressure change does not affect the flow conditions.

Attempts to apply this reasoning to two-phase, one-component flow have met with little success. Most recent investigators (*1* to 3) have employed a single-fluid concept or homogeneous model. It predicts critical flow rates that are lower than experimentally determined ones by a factor as great as six. However, deviations from this model have appeared to be a strong function of quality, with a weak pressure dependence in the 0.01 to 0.15 quality region. Three investigators (*1* to 3) have presented their data in this fashion. Fauske (*4*) attacked the problem with a different approach, which closely predicted the published experimental data. His theoretical treatment, however, is subject to question.

Recently, critical flow models were proposed by Moody (*5*) and by Levy (*6*). Employing the total energy equation solved for flow rate, Moody found that the flow rate maximized when $dG/dP = 0$ and when the slip ratio K was equal to $(V_g/V_f)^{1/3}$. Levy's approach was based on the separated model momentum equation. By equating the static pressure drops in each phase, he was able to relate the mixture quality and void fraction. Using this relationship and $G^2 = -g_c(dP/dV_M)$, he computed critical flow rates for steam-water mixtures. Results of both Moody's and Levy's models agreed closely with published experimental data.

In the following treatment, critical flow is depicted as occurring at the maximum entropy state for constant area flow under a given total energy. The model is intended to apply to adiabatic two-phase systems in thermodynamic equilibrium.

A ONE-DIMENSIONAL APPROACH TO TWO-PHASE HYDRODYNAMICS

Because of its complexity, two-phase, one-component flow is usually treated mathematically in one dimension. Generalized mass, momentum, and energy balance equations are greatly simplified if the following assumptions are made: (1) The flow is one-dimensional. (2) The flow is adiabatic and at steady state.

The conservation equations abstracted from Meyer (7) are listed below in integral form.

Mass:

$$\partial/\partial Z\left(\int_A \rho u_Z\, dA\right) = 0 \tag{1}$$

Momentum:

$$\frac{1}{g_c}\partial/\partial Z\left(\int_A \rho u_Z^2 dA\right) = \frac{A dP}{dZ} - \int_C \tau dL - \left(\int_A \rho dA\right)\frac{g}{g_c}\sin\alpha \tag{2}$$

Mechanical energy:

$$\frac{1}{2g_c}\partial/\partial Z\left(\int_A \rho u_Z^3 dA\right) = -\left(\int_A u_Z dA\right)\frac{dP}{dZ} - GA\frac{JTdS}{dZ} - \left(\int_A \rho u_Z dA\right)\frac{g}{g_c}\sin\alpha \tag{3}$$

Energy:

$$\partial/\partial Z\left(\int_A \rho u_Z H dA\right) = \left[-\partial/\partial Z\left(\int_A \frac{1}{2}\rho u_Z^3 dA\right) - \left(\int_A \rho u_Z dA\right) g\sin\alpha\right]\frac{1}{g_c J} \tag{4}$$

For further simplification of Equations (1) to (4), the following quantities may be defined:

James E. Cruver is with C. F. Braun and Company, Alhambra, California.

Mass flow rate:

$$G = \frac{1}{A} \int_A \rho u_Z \, dA \tag{5}$$

Area average specific volume:

$$V_A = \left(\frac{1}{A} \int_A \rho \, dA \right)^{-1} \tag{6}$$

Momentum average specific volume:

$$V_M = \frac{1}{G^2 A} \int_A \rho u_Z^2 \, dA \tag{7}$$

Kinetic energy average specific volume:

$$V_{KE} = \left[\frac{1}{G^3 A} \int_A \rho u_Z^3 \, dA \right]^{1/2} \tag{8}$$

Velocity-weighted specific volume (homogeneous):

$$V_H = \frac{1}{GA} \int_A u_Z \, dA \tag{9}$$

Flow-weighted enthalpy:

$$\overline{H} = \frac{1}{GA} \int_A \rho u_Z H dA \tag{10}$$

Substituting these definitions back into the conservation equations, we obtain

$$\partial/\partial Z \, (GA) = 0 \tag{11}$$

$$\partial/\partial Z \, (V_M G^2 A) = -g_c A \frac{dP}{dZ} - g_c \int_C \tau dL - \frac{gA}{V_A} \sin \alpha \tag{12}$$

$$\frac{1}{2g_c} \partial/\partial Z \, (G^3 A V_{KE}^2) = -GAV_H \frac{dP}{dZ} - GA \, JT \frac{dS}{dZ} - \frac{GAg}{g_c} \sin \alpha \tag{13}$$

$$\partial/\partial Z \, (G\overline{H}A) = \left[-\frac{1}{2} \partial/\partial Z \, (G^3 A V_{KE}^2) - GAg \sin \alpha \right] \frac{1}{g_c J} \tag{14}$$

Equations (11) to (14) represent the laws of conservation of mass, momentum, and energy for a variable-area, adiabatic, steady state channel flow. If single-phase flow with a flat velocity profile is assumed, $V_A = V_M = V_{KE} = V_H = 1/\rho$. However, these quantities differ slightly when a velocity profile is curved in single-phase flow; they may deviate significantly in two-phase flow.

HOMOGENEOUS AND SEPARATED FLOW MODELS

Two models, homogeneous and separated, are currently used to depict two-phase flow. The homogeneous model treats the mixture as a single fluid whose properties depend upon the relative abundance of each phase. Thus the specific volume and enthalpy of the mixture are given by the expressions

$$V_H = X \, V_g + (1 - X) \, V_f$$

$$\overline{H}_H = X \, H_g + (1 - X) \, H_f$$

Since homogeneous, two-phase flow is but a simple extension of single-phase flow, $V_A = V_M = V_{KE} = V_H$. The model has had moderate success in describing two-phase flow if the density difference between the phases and the total flow rate are low. It does a poor job of predicting liquid-vapor critical flow rates.

It is well known that many flow patterns can exist in two-phase flow. At mass flow rates approaching the critical, one would expect only bubble, annular, or mist flow to be present, according to Baker's correlation (8). The separated flow model was originally intended to depict annular flow, but it has been used successfully to correct for differing phase velocities in other flow regimes as well (9).

Two stream tubes exist according to the separated model. Each is characterized by a cross section normal to the flow, a mass flow rate, a uniform velocity, and a set of physical properties. One recognizes immediately that this is only a simplified approximation. For instance, in mist and bubble flow a spectrum of droplet and bubble velocities exists. If discussion is limited now to a constant area flow passage, Equations (5) through (10) become

$$G = G_g + G_f \tag{15}$$

$$V_A = \left[\frac{1 - R_g}{V_f} + \frac{R_g}{V_g} \right]^{-1} \text{ where}$$

$$R_g = \left[\left(\frac{1 - X}{X} \right) \left(\frac{V_f}{V_g} \right) K + 1 \right]^{-1} \tag{16}$$

$$V_M = \frac{X^2 V_g}{R_g} + \frac{(1 - X)^2 V_f}{1 - R_g} \tag{17}$$

$$V_{KE} = \left[\frac{X^3 V_g^2}{R_g^2} + \frac{(1 - X)^3 V_f^2}{(1 - R_g)^2} \right]^{1/2} \tag{18}$$

$$V_H = (1 - X) \, V_f + X V_g \tag{19}$$

$$\overline{H} = (1 - X) \, H_f + X \, H_g \tag{20}$$

Area, momentum, and kinetic energy average specific volumes may also be written in terms of the slip ratio:

$$V_A = \frac{(1 - X) \, V_f K + X V_g}{(1 - X) \, K + X} \tag{21}$$

$$V_M = \left[\frac{X V_g}{K} + (1 - X) \, V_f \right] [1 + X \, (K - 1)] \tag{22}$$

$$V_{KE} = \left\{ \left[\frac{X V_g}{K} + (1 - X) \, V_f \right]^2 [1 + X \, (K^2 - 1)] \right\}^{1/2} \tag{23}$$

Since the separated model becomes equivalent to the homogeneous model if the slip ratio K equals one, K is a measure of the departure from homogeneous flow. Slip introduces an extra degree of freedom into the flow, and it must be recognized that slip does not affect momentum and kinetic energy in the same manner. Typical behavior of the four defined specific volumes with slip ratio is shown in Figure 1.

Area average specific volume V_A decreases monotonically with slip ratio; however, momentum and kinetic energy average specific volumes do not—each exhibits a minimum. The momentum average specific volume minimizes with respect to slip ratio at $K = (V_g/V_f)^{1/2}$, while V_{KE} reaches its minimum value at $K = (V_g/V_f)^{1/3}$. Vance (9) has shown that the forward momentum of a liquid-vapor stream minimizes with respect to slip ratio when $K = (V_g/V_f)^{1/2}$. Since a higher slip ratio would increase the forward momentum, its presence is highly unlikely.

Kinetic energy also minimizes with slip ratio. At any point in liquid-vapor flow, the separated model kinetic energy is

$$KE = \frac{G^2}{2g_c J} V_{KE}^2 \tag{24}$$

Taking the variation with respect to slip ratio, setting it equal to zero, and solving for K we show that kinetic

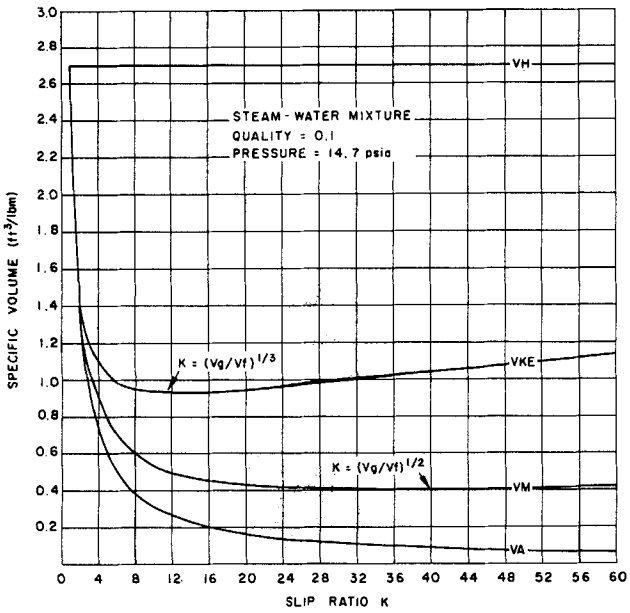

Fig. 1. Effect of slip ratio on mixture specific volume.

energy minimizes with respect to slip ratio when $K = (V_g/V_f)^{1/3}$.

At any cross section, the separated flow energy equation is

$$H^o = XH_g + (1-X)H_f + \frac{G^2 V_{KE}{}^2}{2g_c J} \qquad (25)$$

Taking the variation with respect to K we get

$$\frac{\partial H^o}{\partial K} = \frac{\partial (KE)}{\partial K}$$

Thus, the required total energy for a given flow minimizes with respect to slip ratio when the slip ratio reaches $(V_g/V_f)^{1/3}$. Or, if the total energy is fixed, mass flow rate maximizes with respect to slip ratio when $K = (V_g/V_f)^{1/3}$. Because a higher slip ratio would increase a flow's total energy requirement, a slip ratio greater than $(V_g/V_f)^{1/3}$ would not be expected.

To establish whether or not $(V_g/V_f)^{1/3}$ is truly the maximum attainable slip ratio in separated two-phase flow, one must consider the relationship between slip ratio and entropy production. Equation (13), which relates entropy production by viscous dissipation to the flow variables, will be employed to establish this interconnection. However, it is first important to recognize that Equation (13) implies that even though thermodynamic equilibrium does not truly exist, the equilibrium relationships are valid. Prigogine (*10*) has shown that the domain of validity of the irreversible thermodynamic principle of minimum entropy production is restricted to transport processes which meet the following conditions: linear phenomenological laws, Onsager's reciprocity relations are valid, and phenomenological coefficients may be treated as constants.

Therefore Equation (13) has not yet been shown to be universally true for high-speed flows, where the phenomenological laws are nonlinear and the phenomenological coefficients are not constant. Thus the following treatment is tentative, and it awaits further developments in nonlinear analysis techniques of irreversible thermodynamics. In the interim, comparison of theoretical results with experiment will be used as one test of the approach.

At constant area, the mechanical energy balance, Equation (13), after rearrangement and integration is

$$\Delta S = -\frac{1}{JT_{avg}}\left[\frac{G^2}{2g_c}\Delta V_{KE}{}^2 + \int_1^2 V_H dP + \frac{g}{g_c}\sin\alpha\,\Delta Z\right] \qquad (26)$$

Taking the variation of ΔS with respect to K, we get

$$\frac{\partial \Delta S}{\partial K} = -\frac{G^2}{2g_c J T_{avg}}\frac{\partial (\Delta V_{KE}{}^2)}{\partial K} \qquad (27)$$

Thus the increase in entropy due to slip ratio is directly proportional to $\frac{\partial(\Delta V_{KE}{}^2)}{\partial K}$. By letting ΔV_{KE} represent the difference between separated and homogeneous flow, ΔS is then the entropy difference between the two flow modes.

Since $\partial V_H{}^2/\partial K = 0$, $\frac{\partial(\Delta V_{KE}{}^2)}{\partial K} = \frac{\partial (V_{KE}{}^2)}{\partial K}$. This function is negative in the region $1 < K < (V_g/V_f)^{1/3}$ and equals zero at $K = (V_g/V_f)^{1/3}$. Therefore the entropy of the system increases with slip ratio, reaches a maximum with it at $K = (V_g/V_f)^{1/3}$, and decreases with it at $K > (V_g/V_f)^{1/3}$.

One can generally say that for constant-area separated flow, any change in slip ratio will be in the direction of $(V_g/V_f)^{1/3}$. Initially, if a slip ratio greater than $(V_g/V_f)^{1/3}$ is present, it will tend to be reduced. On the contrary, a slip ratio lower than $(V_g/V_f)^{1/3}$ will tend to increase. However one cannot generally infer that a slip ratio increase above $(V_g/V_f)^{1/3}$ violates the second law of thermodynamics, because the system's entropy may change in other ways.

CRITICAL FLOW EXPRESSION

When a liquid-vapor mixture flows in a pipe, vaporization (sometimes condensation) occurs as the static pressure decreases. Boiling causes a large volume increase and a corresponding acceleration of the two-phase mixture. Specific volume change due to condensation is less than that caused by the static pressure decrease, so the mixture accelerates here too. If the axial pressure profile is steepened by decrease in the downstream pressure, mass flow rate will increase only up to a certain value. Beyond this point, back pressure will have no effect on the flow rate. The maximum is called the *critical flow rate;* the pressure where this condition is reached is labeled the *critical pressure.*

Single-phase critical flow is sometimes described as the maximum entropy state for constant area flow under a given total energy. The familiar fanno line diagrams, originally proposed by Stodola (*11*), point this out. Here, the same description will be applied to liquid-vapor critical flow.

Note that in single-phase flow, critical flow occurs when the stream travels at sonic velocity. This is not true for liquid-vapor critical flow, according to the experimental results of Faletti (*1*) and of Zaloudek (*3*). It is difficult to depict a two-phase mixture, with differing phase velocities, as having a characteristic sonic velocity.

At critical flow $dS = 0$, and the mechanical energy balance Equation (13) is solved for G^2 and constant area flow, giving

$$G^2 = -2g_c V_H\left(\frac{\partial P}{\partial (V_{KE}{}^2)}\right)_S - 2g\sin\alpha\left(\frac{\partial Z}{\partial (V_{KE}{}^2)}\right)_S \qquad (28)$$

Recognizing that the elevation term is very small com-

pared to the reciprocal compressibility term, we can neglect it, leaving

$$G^2 = -g_c V_H \left(\frac{\partial P}{\partial (V_{KE}{}^2)}\right)_S \tag{29}$$

as the critical flow expression for two-phase separated flow.

A slip ratio must be specified to solve Equation (29). It has been shown in the previous section that the system's entropy increase due to slip ratio maximizes when $K = (V_g/V_f)^{1/3}$. To maximize the entropy of the system, $(V_g/V_f)^{1/3}$ must be the slip ratio at critical flow. Evaluation of the partial derivative in Equation (29) yields the following expression for critical flow:

$$G = \left\{ \frac{-g_c V_H}{V_f[1 + X(K^2-1)]^2 \left[\frac{X}{K}\left(\frac{\partial V_g}{\partial P}\right)_S + 3/2\, V_f (K^2-1)\left(\frac{\partial X}{\partial P}\right)_S + (1-X)\left(\frac{\partial V_f}{\partial P}\right)_S \right]} \right\}^{1/2} \tag{30}$$

Equation (30) indicates the critical flow rate to be as a function of individual phase specific volumes, mixture quality, and their partial derivatives with respect to pressure at constant entropy. Evaluation of the fluid properties in Equation (30) depends upon whether or not the liquid-vapor mixture is in thermodynamic equilibrium. This subject is treated in reference *12*. It is assumed that thermodynamic equilibrium exists in this development. Therefore, properties become a function of pressure only and the partial derivative of quality with respect to pressure at constant entropy is

$$\left(\frac{\partial X}{\partial P}\right)_S = -\frac{1}{S_g - S_f}\left[\frac{dS_f}{dP} + X\frac{d(S_g - S_f)}{dP}\right] \tag{31}$$

Critical flow rates for steam-water mixtures under thermodynamic equilibrium conditions given by Equation (30) are plotted in Figure 2 vs. total energy, with pressure and quality as parameters.

In reference *12*, a critical flow expression was developed from the momentum Equation (12). By solving it for G^2 under constant area flow, the following is obtained:

$$G^2 = -g_c \frac{\partial P}{\partial V_M} - \frac{g_c}{\left(\frac{\partial V_M}{\partial Z}\right) A}\int_C \tau dL - \frac{g}{\left(\frac{\partial V_M}{\partial Z}\right) V_A}\sin\alpha \tag{32}$$

As mass flow rate increases, acceleration pressure drop overshadows both frictional and gravitational pressure drops. A limit to this process would be the complete disappearance of the frictional and gravitational terms. Since frictionless, adiabatic flow connotes isentropic flow

$$G^2 = -g_c \left(\frac{\partial P}{\partial V_M}\right)_S \tag{33}$$

If this equation were regarded alone, G would maximize when $K = (V_g/V_f)^{1/2}$. However, entropy considerations dictate that K max $= (V_g/V_f)^{1/3}$. Evaluation of Equation (33) gives the following expression for critical flow:

$$G = \left[\frac{-g_c K}{A\left(\frac{\partial V_g}{\partial P}\right)_S + B\left(\frac{\partial X}{\partial P}\right)_S + C\left(\frac{\partial V_f}{\partial P}\right)_S}\right]^{1/2} \tag{34}$$

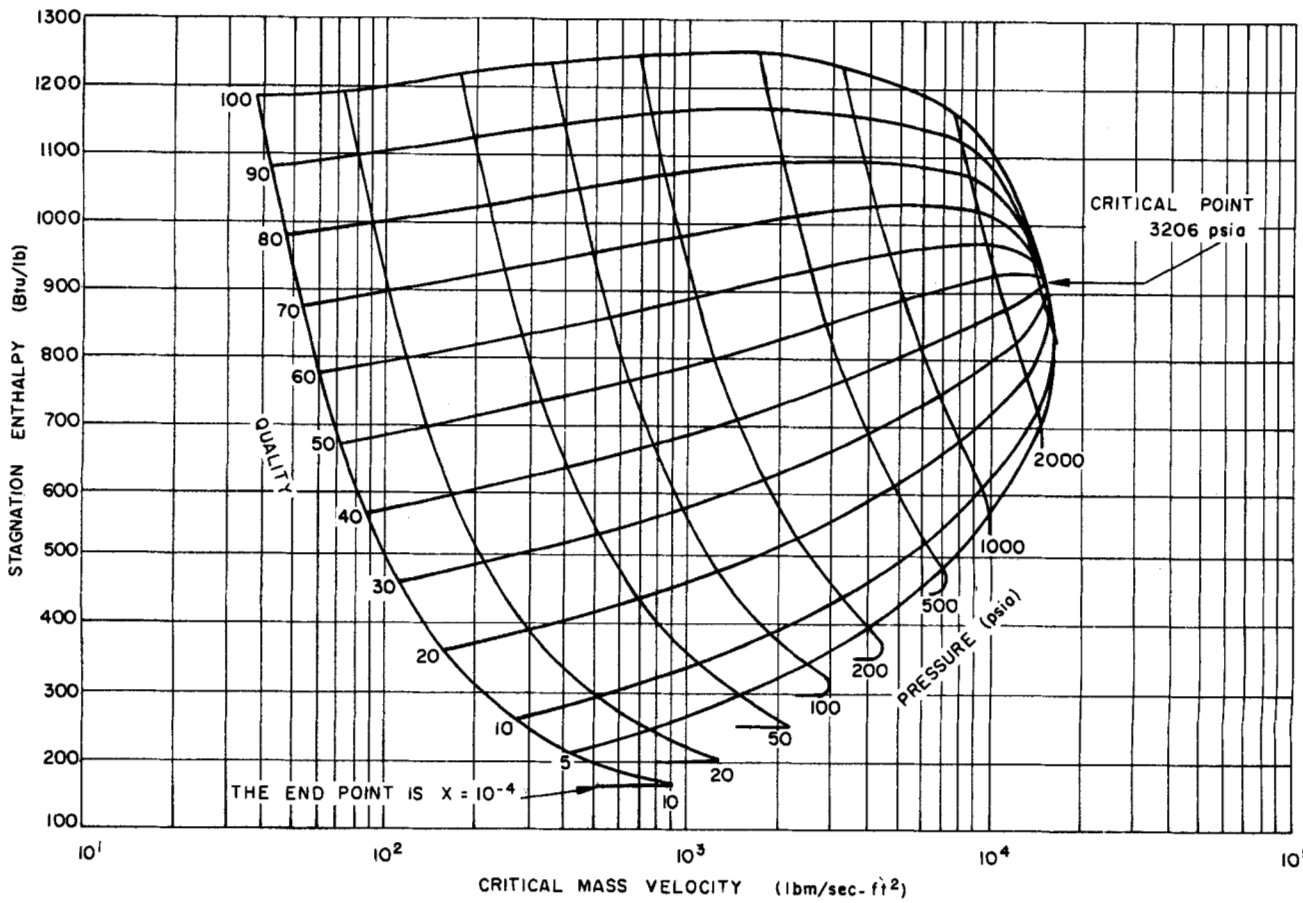

Fig. 2. Steam-water critical flow rates by the maximum slip ratio model.

where

$$A = X\left[1 + \frac{(K-1)}{3K}\left[X(3K+1) - 1\right]\right]$$

$$B = V_g\left[1 + 2X(K-1)\right] + V_f K\left[(1-2X)(K-1) - 1\right]$$

$$C = (1-X)\left[1 + X(K-1)\left(1 + \frac{K^2}{3}\right)\right]$$

The momentum model critical flow equation was incorrect when presented in reference 12. The error has been rectified here. Moody's model was derived from the total energy balance Equation (25). The ratio of Moody's expression to Equation (30) is

$$\frac{G_{\text{Moody}}}{G_{\text{Equation (30)}}} = \frac{J}{V_H}\left(\frac{\partial \bar{H}}{\partial P}\right)_S$$

Because the conservation equations should be consistent, critical flow rates calculated by either of the three approaches should be equal. But the critical flow expressions are not equal, which indicates a serious deficiency in the separated model when applied to liquid-vapor critical flow.

A CRITIQUE OF THE ISBIN-FAUSKE MODEL

Fauske (4) presented a model for two-phase critical flow by using a radically different approach. His reasoning is outlined and commented upon in the following discussion. He made five key assumptions in the development of the model.

1. Separated flow (annular flow pattern)
2. Thermodynamic equilibrium between liquid and vapor phases
3. Critical flow is attained when $dG/dP = 0$
4. The absolute value of the pressure gradient reaches a finite (rather than infinite) maximum for a given flow rate and quality at the point of critical flow

$$\left|\frac{dP}{dZ}\right|_{G,\,X} = \{\max\}\ \text{Finite}$$

5. Irreversibility can be accounted for by a friction factor defined as

$$F = \frac{2\,g_c D \int_c \tau dL}{A\,G^2\,V_M}$$

After employing assumption 5 and after neglecting the gravitational term, the momentum Equation (12) becomes

$$-\frac{dP}{dZ} = \frac{G^2}{g_c}\left(\frac{\partial V_M}{\partial Z} + \frac{f\,V_M}{2D}\right) \qquad (35)$$

Because of assumption 4, the right-hand side of Equation (35) must reach a finite maximum. Fauske reasoned that the slip ratio, being the only unrestricted variable, maximized the acceleration and frictional pressure drops.

Taking the variation of Equation (35) with respect to K, we obtain

$$\partial/\partial Z\left(\frac{\partial V_M}{\partial K}\right) + \frac{f}{2g_c}\left(\frac{\partial V_M}{\partial K}\right) + \frac{V_M}{2D}\left(\frac{\partial f}{\partial K}\right) = 0 \qquad (36)$$

where

$$\frac{\partial V_M}{\partial K} = X(1-X)\left(V_f - \frac{V_g}{K^2}\right)$$

and a maximum exists.

Fauske stated that $\partial V_M/\partial K = \partial f/\partial K = 0$ was a solution to Equation (36), and arrived at $K = (V_g/V_f)^{1/2}$ as the slip ratio that would maximize the pressure gradient. He obtained $(\partial f/\partial K)$ by graphing average friction factor from his experimental data vs. slip ratio. He found that the friction factor maximized with respect to K when $K = (V_g/V_f)^{1/2}$ for the experimental runs he investigated. The rest of Fauske's justification of his fourth assumption was erroneous for two reasons. First, $\partial V_M/\partial K = 0$ represents a minimum, not a maximum, because $\partial^2 V_M/\partial K^2 = 2X(1-X)V_g/K^3$ is always positive. Second, the assumption that $\partial V_M/\partial K = \partial f/\partial K = 0$ solves Equation (36) is not absolutely correct. The first term is $\partial/\partial Z\,(\partial V_M/\partial K)$. When $\partial V_M/\partial K$ reaches zero at a given point, the derivative does not necessarily equal zero at that point. The behavior of $\partial/\partial Z\,(\partial V_M/\partial K)$ at critical flow cannot presently be determined analytically, however, it can be approximated by the scheme discussed in the following paragraphs.

Substitution of the expression for $\partial V_M/\partial K$ into the first term of Equation (36) gives

$$\partial/\partial Z\left[X(1-X)\left(V_f - \frac{V_g}{K^2}\right)\right] = 0 \qquad (37)$$

This indicates that at $Z = 0$

$$X(1-X)\left(V_f - \frac{V_g}{K^2}\right) = \text{constant} \qquad (38)$$

Notice that Equation (38) is tantamount to saying that at $Z = 0$

$$K^2 = \frac{X(1-X)\,V_g}{X(1-X)\,V_f - \text{constant}} \qquad (39)$$

Since the constant is arbitrary, Equation (38) stipulates a slip ratio expression, not a specific value. This shows that

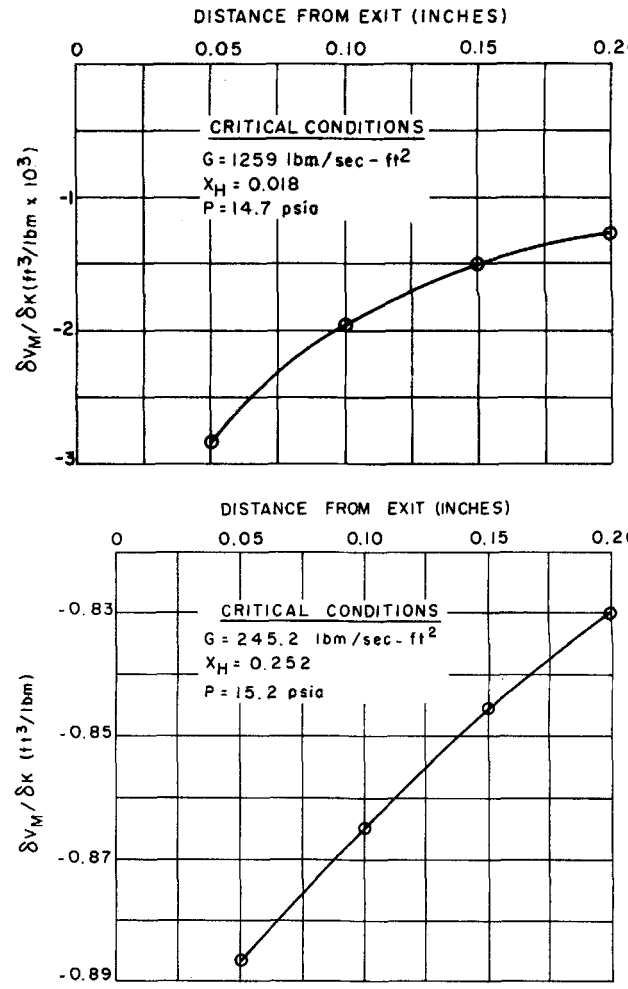

Fig. 3. Variation in V_M with respect to K vs. distance.

TABLE 1. RECENT CRITICAL FLOW STUDIES: RANGE OF PARAMETERS

Investigator	Exit quality	Exit pressure, lb./sq. in. abs.	Critical flow rate, lb.$_m$/(sec.)(sq. ft.)	Pipe size and length, in.	Distance from exit of last pressure tap (No. of equiv. diameters)
Faletti (*1*)	0.001 to 0.975	26 to 106	126 to 6,215	0.574 I.D., 0.188 and 0.375 O.D. center rods, length of 35.14, 21.31, 8.98, 0.5313	At exit ±0.04 to 0.08
Fauske (*4*)	0.010 to 0.700	40 to 360	500 to 4,300	0.269, 0.125, 0.4825 I.D., lengths of 56.25 and 110	1
Zaloudek (*3*)	0.004 to 0.990	40 to 110	100 to 1,000	0.520 and 0.625 I.D., lengths to 48	0.06
Cruver(*12*)	0.018 to 0.971	14.7 to 40.5	88.6 to 1,259	0.512 I.D., length 24	0.02

$\partial/\partial Z\ (\partial V_M/\partial K) = 0$ may be satisfied by an infinite number of slip ratios as given by Equation (39).

Slip ratio data have not yet been published at critical flow, but Vance (*9*) collected and restrictively correlated slip ratio data at flow rates up to $G/G_{\text{critical}} = 0.95$. By using Vance's slip ratio correlation within the range of his experimental data, and a critical flow pressure profile from reference *12*, $\partial V_M/\partial K$ was determined as a function of Z (see Figure 3). If $\partial/\partial Z\ (\partial V_M/\partial K)$ tended toward zero as $Z \rightarrow 0$, one could state that Equation (36) is valid even though an absolute maximum with respect to slip ratio is not present.

Examination of Figure 3 reveals that $\partial/\partial Z\ (\partial V_M/\partial K)$ increases as Z approaches zero. This, while not giving conclusive proof, strongly indicates that Equation (36) is invalid. Thus, one concludes that dP/dZ does not attain a finite maximum in two-phase critical flow because of a slip ratio variation.

COMPARISON WITH EXPERIMENTAL DATA

Steam-water critical flow predictions by the maximum slip ratio model are compared with the combined data of Faletti (*1*), Fauske (*4*), Zaloudek (*3*), and Cruver (*12*). Parameter ranges of the experimenters are indicated in Table 1. Though the investigators explored different regions of pressure, there is close agreement in areas of overlap. The critical flow data also show reasonable consistency when plotted vs. pressure and quality.

All four investigators measured critical flow of steam-water mixtures in constant-area conduits. Streams of steam and water were intimately mixed in varying proportions prior to entering the test section. Friction and acceleration pressure decreases in the flow direction caused the maximum velocity, hence the critical condition, to occur at the pipe's end.

Exit pressures were determined by extrapolation from a series of static pressure measurements near the end of each test section. All data were subject to some error because the pressure profile near the exit is very steep (up to 250 lb./sq.in./in. in reference *12*). Earlier investigators (*2*) did not determine the pressure profile in the steep region, so their results are not included in this comparison. Table 1 lists distance of the last pressure tap from the exit for the four sets of critical flow data employed here.

Each experimenter ascertained exit quality by heat balance, by employing a flow model to determine kinetic energy. Fortunately, differences between exit quality calculated by the homogeneous and separated models are quite small. Qualities based upon the homogeneous model are employed in this analysis. If the separated model had been used instead, agreement between experimental and predicted critical flow rates would be slightly closer at low qualities and nearly the same at high qualities.

Combined critical flow data of references *1*, *3*, *4*, and *12* are presented in Figures 4 through 6. These plots indicate critical flow rate as a function of pressure with a quality parameter. Experimental data are grouped into quality ranges, and the maximum slip ratio model prediction at the midpoint of each range is shown for thermodynamic equilibrium between the phases. Both approaches to the maximum slip ratio model (momentum and mechanical energy equations) are included on the graphs. Predicted flow rates follow well the pressure behavior of the experimental data; deviations appear to be a function of quality only. The critical flow rates of the mechanical energy equation approximate the experimental data more closely than those of the momentum equation.

Table 2 indicates average deviation between mechanical energy balance predicted and experimental critical flow rates for each quality range. Predicted values are too low at high qualities and too high at low qualities. The average percentage difference from all the experimental data is -8.5%.

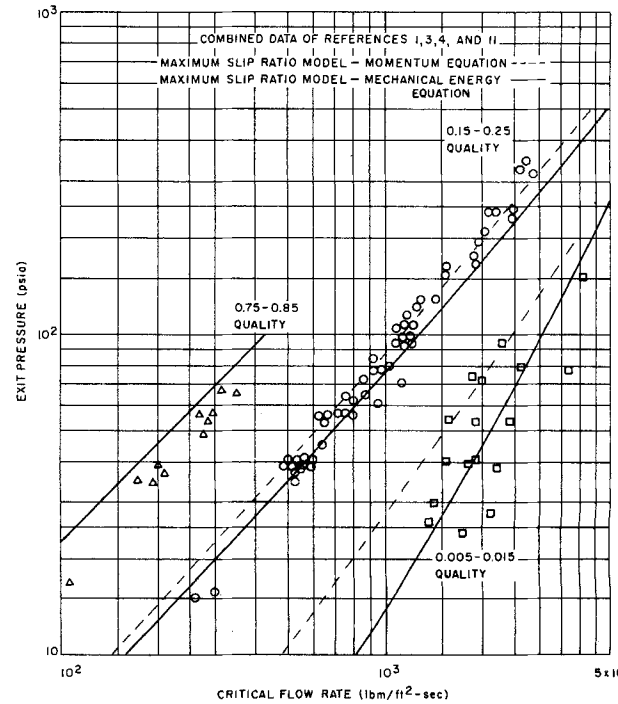

Fig. 4. Critical flow rate vs. exit pressure. Quality ranges 0.005 to 0.015, 0.15 to 0.25, 0.75 to 0.85.

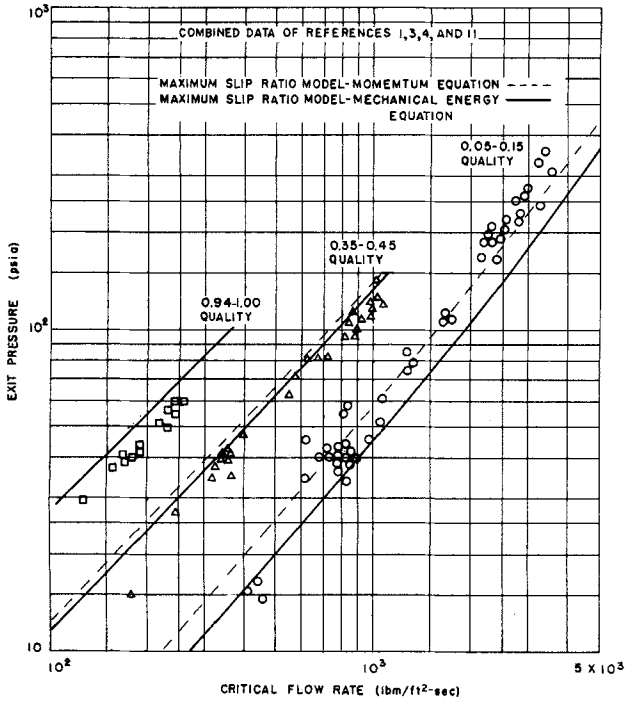

Fig. 5. Critical flow rate vs. exit pressure. Quality ranges 0.05 to 0.15, 0.35 to 0.45, 0.94 to 1.00.

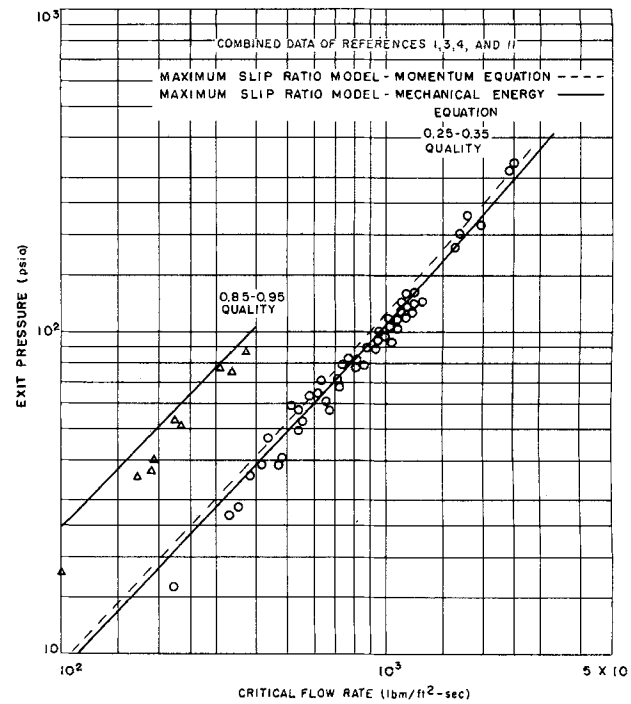

Fig. 6. Critical flow rate vs. exit pressure. Quality ranges 0.25 to 0.35, 0.85 to 0.95.

Critical flow rates predicted by Equation (30) are compared with large diameter (6- and 8-in.) pipe steam-water critical flow data reported by James (*13*) in Figure 7. There is good agreement at higher qualities, but the model predicts higher than the experimental flow rates at low qualities.

Why isn't the agreement between predicted and experimental critical flows closer? This question cannot yet be definitely answered. However, three factors may contribute. Drop size, if below 10^{-7} ft., may cause a significant proportion of the system's total energy to reside in the interfaces between the phases. This effect, which has not yet been determined at critical flow, should decrease the mixture quality and thus increase the critical flow rate. The phenomenon should have the most prominence at high qualities.

Reference *12* indicates that metastable states are present in critical steam-water flow. Both super heating (to 14.0°F.) and supercooling (to 7.5°F.) were indicated by simultaneous temperature and pressure measurements. If these data were incorporated into the maximum slip ratio model, they would cause the model to predict higher critical flow rates throughout most of the quality spectrum.

Another possibility dwells with the slip ratio. Vance's results (9) show that K is a strong function of quality, pressure, and the ratio of the mass velocity to the critical mass velocity at G/G_c values approaching unity. Whether or not the slip ratio actually reaches $(V_g/V_f)^{1/3}$, which is quality independent, remains to be experimentally determined.

COMPARISON OF TWO-PHASE AND SINGLE-PHASE CRITICAL FLOW

Mathematically speaking, the differences between two- and single-phase critical flow are not great. Both are given by the square root of the reciprocal compressibility at constant entropy. Important mathematical differences are caused by slip, vaporization rate, and the inequality of critical flow rates calculated by the momentum and mechanical energy equations. However, many investigators have noticed other important contrasts.

Faletti (*1*), Fauske (*4*), and Zaloudek (3) each observed that the approach to two-phase critical flow was asymptotic. Faletti concluded that below 50% steam, complete sonic choking may not be achieved. Zaloudek measured the effects of a back pressure perturbation when the differential pressure was as high as 100 lb./sq.in. These observations clearly point out that additional phenomena, not included in the limiting mathematical expression, contribute significantly to two-phase critical flow.

An important difference between gas and vapor-liquid flow lies in the relative importance of the frictional term in the momentum equation. It is much larger in two-phase flow than with either phase flowing alone. Therefore, a greater total pressure drop is necessary for a given sum of accelerational and gravitational pressure drops. Also, in vapor-liquid flow at equal levels of the other parameters, friction pressure drop increases as quality decreases (see reference *14*).

To characterize the difference more thoroughly, Equation (32) is restated:

Table 2. Comparison of Maximum Slip Ratio Mechanical Energy Model Prediction with Experimental Critical Flow Data

% Quality range	No. of data points	Average percentage difference $\frac{G_{exp.}-G_{pred.}}{G_{exp.}} \times 100$
94 to 100	14	13.2
85 to 95	9	11.6
75 to 85	11	13.1
65 to 75	13	15.1
55 to 65	31	10.5
45 to 55	22	9.8
35 to 45	37	5.5
25 to 35	56	—1.1
15 to 25	61	—10.4
5 to 15	53	—27.3
0 to 5	69	—35.2

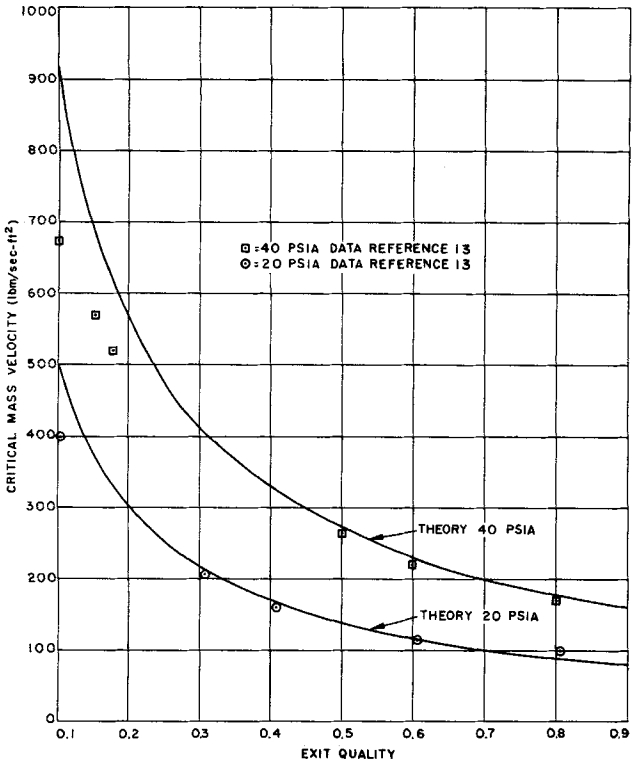

Fig. 7. Comparison of maximum slip ratio model predicted critical flow rates with the experimental data of James.

$$G^2 = -g_c \frac{\partial P}{\partial V_M} - \frac{g_c}{\left(\frac{\partial V_M}{\partial Z}\right) A} \int_C \tau dL - \frac{g}{\left(\frac{\partial V_M}{\partial Z}\right) V_A} \sin \alpha$$

As the maximum flow rate is approached with gas flow, $(\partial V_M/\partial Z)$ tends to infinity, which reduces the already small frictional and gravitational terms to almost zero. This situation is accomplished with relatively small differences between the throat and back pressures in gas flow. If the reasoning behind the maximum slip ratio model is correct, $(\partial V_M/\partial Z)$ also moves toward infinity as two-phase critical flow is approached. Since the frictional and gravitational terms are greater, a larger difference between the throat and back pressure is required to reach fully critical flow.

The approach to two-phase critical flow is further complicated by relative velocity. Other factors being equal, slip lowers the acceleration pressure drop. Vance's (9) results show that slip ratio markedly increases as critical flow is approached. Figure 3 indicates that $\partial/\partial Z$ $(\partial V_M/\partial K)$ also increases as $Z \rightarrow 0$. Since $(\partial V_M/\partial K)$ is always negative, $(\partial V_M/\partial Z)$ is lowered by the slip ratio. Thus, even when slip's increased frictional pressure drop is ignored, relative velocity serves to augment the importance of frictional pressure drop as critical flow is approached. Therefore, slip contributes to the asymptotic approach to critical flow.

SUMMARY OF CONCLUSIONS

1. To describe adequately separated two-phase flow by a one-dimensional approach, four different mixture specific volumes must be defined. One is based on an area average; the second is based on a momentum average; the third is based on a kinetic energy average; and the last is based on a velocity average.

2. Increased relative velocity between the phases initially lowers all specific volumes except the velocity average. The momentum average specific volume minimizes when the slip ratio equals $(V_g/V_f)^{1/2}$, while the kinetic energy average specific volume reaches its minimum value at a slip ratio of $(V_g/V_f)^{1/3}$. Area average specific volume does not minimize with slip ratio.

3. Because a higher slip ratio decreases the entropy of a closed system, $(V_g/V_f)^{1/3}$ is the maximum slip ratio attainable in two-phase critical separated flow.

4. A new critical flow model based on isentropic separated flow and the maximum slip ratio was developed and compared with the steam-water critical flow data of four investigators. While the predicted flow rates followed well the pressure behavior of the experimental data, they were too low at high qualities and too high at low qualities.

5. Differences in the approach to critical flow between a gas and a vapor-liquid stream appear to be caused by the latter's increased frictional and gravitational pressure drops and relative velocity effects.

ACKNOWLEDGMENT

The authors are indebted to W. H. Vance, who carefully reviewed this work and offered several valuable suggestions. This study was financed by a U. S. Atomic Energy Commission grant, which is gratefully acknowledged.

NOTATION

A = cross-sectional flow area, sq.ft.
C = wetted perimeter, ft.
D = diameter, ft.
f = friction factor
G = mass flow rate, $lb._m/(sq.ft.)(sec.)$
g = acceleration of gravity, $ft./sec.^2$
g_c = universal gravitational constant = 32.174
H = enthalpy, $B.t.u./lb._m$
$\bar{H}$ = flow-weighted or mixing cup enthalpy, $B.t.u./lb._m$
H^o = stagnation enthalpy, $B.t.u./lb._m$
J = mechanical equivalent of heat = $(778\ ft.)(lb._f)/B.t.u.$
K = slip ratio, u_g/u_f
KE = kinetic energy, $B.t.u./lb._m$
L = circumferential distance, ft.
P = static pressure, lb./sq.in.abs.
R = fraction of the cross-sectional area occupied by a phase
S = entropy, $B.t.u./(lb._m)(°F.)$
T = temperature, °R.
u = velocity, ft./sec.
V = specific volume, $cu.ft./lb._m$
W = mass rate, $lb._m/sec.$
X = quality = W_g/W
Z = axial distance, ft.

Greek Letters

α = inclination angle from horizontal
ρ = density, $lb._m/cu.ft.$
τ = shear stress, $lb._f/sq.ft.$

Subscripts

A = area average
avg = average
f = liquid
g = vapor
H = homogeneous model
KE = kinetic energy average
M = momentum average
Z = direction

LITERATURE CITED

1. Faletti, D. W., and R. W. Moulton, *A.I.Ch.E. J.*, 9, 247 (1963).

2. Isbin, H. S., J. E. Moy, and A. J. R. Cruz, *ibid.*, 3, 361-365 (1957).
3. Zaloudek, F. R., *H W-68934 Rev.*, Hanford Atomics Works (1961).
4. Fauske, H. K., Sc.D. thesis, Univ. Trondheim, Norway (1961); also *ANL 6633*.
5. Moody, F. J., *Trans. Am. Soc. Mech. Engrs.*, **87C**, 134 (1965).
6. Levy, S., *ibid.*, 53.
7. Meyer, J. E., *WAPD-BT-20* (1960).
8. Baker, O., *Oil Gas J.*, **53**, No. 12, 185 (1954).
9. Vance, W. H., Ph.D. thesis, Univ. Washington, Seattle (1962).
10. Prigogine, I., "Introduction to Thermodynamics of Irreversible Processes," Interscience, New York (1955).
11. Stodola, A., "Steam and Gas Turbines," McGraw-Hill, New York (1927).
12. Cruver, J. E., Ph.D. thesis, Univ. Washington, Seattle (1963).
13. James, R., *Proc. Inst. Mech. Engrs.*, (1962).
14. Martinelli, R. C., and D. B. Nelson, *Trans. Am. Soc. Mech. Engrs.*, **70**, 695 (1948).

Manuscript received January 8, 1965; revision received May 27, 1966; paper accepted May 31, 1966. Paper presented at A.I.Ch.E. Houston meeting.

Vapor-Liquid Equilibrium for the System Hydrogen—Benzene—Cyclohexane—*n*-Hexane

ALAN J. BRAINARD and G. BRYMER WILLIAMS

University of Michigan, Ann Arbor, Michigan

This paper presents vapor-liquid equilibrium data for the system hydrogen–benzene–cyclohexane–*n*-hexane over the pressure range of 500 to 2,000 lb./sq.in.abs. and the temperature range of 200° to 300°F. Experimental equipment was constructed that was capable of operating at pressures of 3,000 lb./sq.in.abs. and at temperatures of 400°F. A static equilibrium cell, which had a sample port for both the liquid and vapor phases, was employed. Separation of the hydrogen from the hydrocarbons by means of a liquid nitrogen cold trap was utilized before performing the hydrocarbon analyses on a mass spectrometer. Three hydrocarbon mixtures were charged to the equilibrium cell, and for each charge, isotherms of 200°, 250°, and 300°F. were run for equilibrium pressures of 500, 1,000, 1,500 and 2,000 lb./sq.in.abs. These thirty-six quaternary equilibrium runs resulted in a total of one hundred and forty-four equilibrium data points. In addition, four binary equilibrium runs were determined both for the hydrogen-benzene and hydrogen-cyclohexane systems. A modified version of the Chao-Seader correlation was used to predict the data. This correlation was able to predict all the quaternary equilibrium ratios with an average deviation of 4.86%.

The need for basic data on the vapor-liquid equilibrium in hydrogen-hydrocarbon systems has become more important recently, especially in the design of commercial hydrocracking units. The bulk of the published literature in this area has appeared within the past twenty years, and it is likely that there is more interest and activity in this area than ever before.

The wide variety of possible hydrogen-hydrocarbon systems, as well as temperature and pressure conditions that may be of interest, points out the need of a prediction technique that will handle these systems. Physical chemists and physicists have been developing models of the gaseous and liquid states that enable one to predict the properties of these states.

For the most part, engineers have turned to empirical approaches to the subject, and a number of generalized charts have been developed. The NGAA charts (*1*), the Kellogg charts (*2*), and the chart of Hougen et al. (*3*) are representative of these correlations.

Hydrogen-hydrocarbon systems present interesting experimental challenges. Over quite wide temperature and pressure conditions one is dealing with very small quantities of some of the substances in the system in each of the equilibrium phases. Under the temperature and pressure conditions of this investigation, small hydrogen liquid phase concentrations and small hydrocarbon vapor phase concentrations resulted at equilibrium. It is felt that the experimental approach presented in this paper avoids some of the inherent difficulties present in a normal analysis scheme.

EQUIPMENT

An overall schematic representation of the experimental apparatus is shown in Figure 1. For the sake of description, the system will be divided into three sections: the charging section, the equilibrium section, and the sampling section.

Alan J. Brainard is with Esso Research Laboratories, Baton Rouge, Louisiana.